

# UC San Diego

## UC San Diego Previously Published Works

### Title

Apo-hemoglobin-haptoglobin complexes attenuate the hypertensive response to low-molecular-weight polymerized hemoglobin

### Permalink

<https://escholarship.org/uc/item/5011d7vv>

### Journal

Blood Advances, 4(12)

### ISSN

2473-9529

### Authors

Belcher, Donald A

Munoz, Carlos

Pires, Ivan S

et al.

### Publication Date

2020-06-23

### DOI

10.1182/bloodadvances.2020002045

Peer reviewed

# Apo-hemoglobin-haptoglobin complexes attenuate the hypertensive response to low-molecular-weight polymerized hemoglobin

Donald A. Belcher,<sup>1</sup> Carlos Munoz,<sup>2</sup> Ivan S. Pires,<sup>1</sup> Alexander T. Williams,<sup>2</sup> Pedro Cabrales,<sup>2</sup> and Andre F. Palmer<sup>1</sup>

<sup>1</sup>William G. Lowrie Department of Chemical and Biomolecular Engineering, The Ohio State University, Columbus, OH; and <sup>2</sup>Department of Bioengineering, University of California San Diego, La Jolla, CA

## Key Points

- Hp increases the relative size of LMW polymerized Hb molecules.
- Administration of the apoHb-Hp complex normalizes systemic and microcirculatory hemodynamics after the transfusion of LMW polymerized Hb.

Polymerized hemoglobin (PolyHb) is a promising hemoglobin (Hb)-based oxygen carrier currently undergoing development as a red blood cell substitute. Unfortunately, commercially developed products are composed of low-molecular-weight (LMW) PolyHb molecules, which extravasate, scavenge nitric oxide, and result in vasoconstriction and hypertension. The naturally occurring Hb-scavenging species haptoglobin (Hp), combined with the purified heme-scavenging species apo-hemoglobin (apoHb), is a potential candidate to alleviate the pressor effect of PolyHb. This study evaluated the protective activity of administering the apoHb-Hp complex to mitigate the vasoactive response induced by the transfusion of LMW PolyHb. Hp binding to PolyHb was characterized *in vitro*. The effectiveness of apoHb-Hp administration on reducing the vasoconstriction and pressor effects of PolyHb was assessed by measuring systemic and microcirculatory hemodynamics. Transfusion of LMW PolyHb to vehicle control pretreated animals increased mean arterial pressure while decreasing arteriole diameter and functional capillary density. However, transfusion of LMW PolyHb to apoHb-Hp pretreated animals prevented changes in mean arterial pressure, heart rate, arteriole diameter, blood flow, and functional capillary density relative to before transfusion. These results indicate that the increased size of PolyHb after binding to the apoHb-Hp complex may help compartmentalize PolyHb in the vascular space and thus reduce extravasation, nitric oxide scavenging, and toxicity responsible for vasoconstriction and systemic hypertension.

## Introduction

Closure of blood donation centers and exclusions in blood donor pools have resulted in blood shortages during the recent outbreak of severe acute respiratory syndrome coronavirus 2.<sup>1-3</sup> A 2017 computer simulation of an influenza outbreak in the United States predicted that >541 000 units of blood might be lost at the end of a 48-week influenza pandemic with a 65% reduction in blood donation rates.<sup>4</sup> Furthermore, current red blood cell (RBC) donation trends and extended social distancing guidelines have resulted in dramatically reduced blood donation rates due to mass cancellation of blood drives, which can account for up to 80% of blood donations.<sup>2,3</sup> This deficit in the blood supply emphasizes the need for an RBC substitute when RBC units are not available due to deficits in the blood supply chain. Unfortunately, there are currently no RBC substitutes approved for clinical application.

The presence of low-molecular-weight (LMW) hemoglobin (Hb) species in previous generations of Hb-based oxygen (O<sub>2</sub>) carriers (HBOCs) restricted their application as RBC substitutes.<sup>5</sup> Among the myriad of strategies that can produce HBOCs, using glutaraldehyde cross-linking to form polymerized

Hb (PolyHb) remains popular due to its low cost and excellent scalability. However, commercially developed PolyHbs, HBOC-201 (Biopure Corporation, Cambridge, MA) and PolyHeme (Northfield Laboratories Inc., Northfield, IL), primarily contained fractions of material  $\leq 250$  kDa.<sup>6</sup> LMW PolyHb and unpolymerized Hb extravasate into the interstitial space where they scavenge nitric oxide (NO), resulting in vasoconstriction and systemic hypertension.<sup>7-10</sup> Moreover, free heme release from HBOCs can also lead to systemic toxicity.<sup>11,12</sup> Previously, we determined that increasing the molecular weight (MW) of PolyHb by increasing the molar ratio of glutaraldehyde to Hb attenuated hypertension and renal injury.<sup>13</sup> However, LMW polymers comprise up to 40% of these PolyHb solutions. Unfortunately, removal of these LMW polymers would significantly reduce the yield of PolyHb.<sup>14</sup> Alternatively, recent strategies to mitigate hypertension have used adenosine and nitroglycerin to attenuate the hypertensive response of HBOC-201.<sup>7</sup> Although effective at controlling systemic hypertension, administration of adenosine and nitroglycerin must be carefully controlled to prevent hypotension.<sup>15,16</sup>

Instead, we propose that using naturally occurring mechanisms of Hb detoxification is a potential strategy to mitigate systematic hypertension resulting from the presence of LMW PolyHb in the circulation. The naturally occurring Hb-scavenging protein, haptoglobin (Hp), plays a pivotal role in detoxifying stroma-free Hb in the blood.<sup>17</sup> Previous studies showed that Hp administration normalizes vascular NO signaling after hemolysis.<sup>18,19</sup> Recently, we determined that Hp preferentially binds to LMW PolyHb (MW  $< 256$  kDa).<sup>14</sup> By binding to Hp, the MW of LMW PolyHb is effectively increased. This increase in molecular size may reduce tissue extravasation and subsequent NO scavenging by PolyHb. An illustration of this potential detoxification mechanism is shown in Figure 1.

The second component of stroma-free Hb detoxification is hemopexin, which scavenges heme that is released from stroma free Hb after Hb auto-oxidation.<sup>19,20</sup> By isolating heme within the hemopexin complex, the heme is unable to catalyze oxidative reactions with blood and tissue components, thus preventing lipid, protein, and nucleic acid oxidation. A potential low-cost alternative to hemopexin is heme-free apohemoglobin (apoHb). This molecule is able to scavenge free heme due to its specificity for heme and the highly hydrophobic nature of its vacant heme-binding pocket.<sup>21,22</sup> Combining apoHb with Hp results in a protein complex (apoHb-Hp) that may be able to scavenge both Hb and heme in the plasma.<sup>18</sup>

Because of its ability to compartmentalize stroma-free Hb and scavenge free heme, we hypothesized that administration of the apoHb-Hp complex would reduce hypertension that results from the transfusion of LMW PolyHb. Hp binding to LMW PolyHb was confirmed in vitro with stop-flow fluorescence spectrometry and size exclusion chromatography. Mean arterial pressure (MAP) was used as an indicator of reduced hypertension. In addition, intravital microscopy was used to examine how administration of apoHb-Hp influences functional capillary density (FCD), vascular tone, and blood flow after PolyHb administration.

## Methods

### PolyHb synthesis and biophysical properties

The Hb used in this study was purified from human RBCs via tangential flow filtration, as described by Palmer et al.<sup>23</sup> Hb was polymerized with glutaraldehyde under complete deoxygenation in

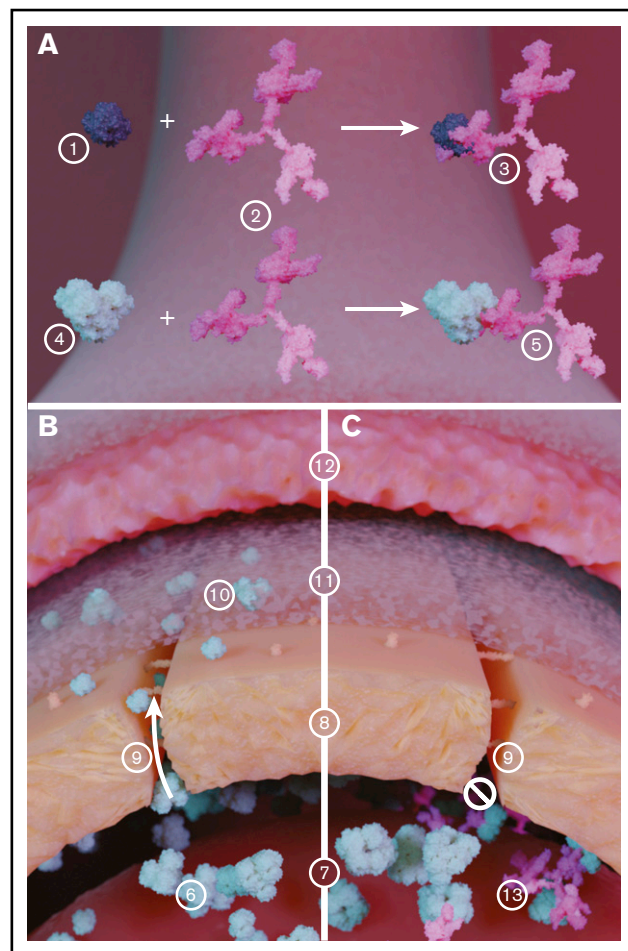


**Figure 1. Illustration of the role of Hp in inhibiting extravasation of LMW**

**PolyHb species.** (A) Hb (1) binds with Hp (2), which significantly increases the size of the resulting Hb-Hp complex (3). Similarly, PolyHb (4) can bind with Hp (2) to form a PolyHb-Hp complex with increased molecular diameter. (B) In circulation, LMW PolyHb (6) can freely extravasate from the blood (7) through the endothelial cell wall (8) via the endothelial gap junction (9). Once past the endothelial wall, the extravasated PolyHb (10) accumulates in the intima (11) where it scavenges the NO produced by the endothelial cells that regulate smooth muscle cell (12) contraction. (C) When PolyHb binds to Hp, the resulting PolyHb-Hp complexes (13) are too large to pass through the endothelial gap junction. This effectively limits PolyHb extravasation into the tissue space and NO scavenging.

the tense quaternary state at a 25:1 molar ratio of glutaraldehyde to Hb.<sup>14</sup> After polymerization, PolyHb was clarified, purified, and buffer exchanged into a modified Ringer's lactate solution by using tangential flow filtration. Modified polyester sulfone hollow fiber filters with an MW cutoff of 100 kDa were used to remove unpolymerized Hb from solution. The PolyHb solution was concentrated to 12 g/dL. The cyanomethemoglobin method was used to measure the Hb concentration and the methemoglobin (metHb) level of Hb/PolyHb solutions.<sup>24,25</sup> The size distribution of PolyHb, according to particle volume, was measured by using dynamic light scattering (BS-200SM; Brookhaven Instrument Inc. Holtsville, NY). The rheology of PolyHb solutions was measured by using a DV3T-CP cone and plate rheometer (Brookfield AMETEK, Middleboro, MA) with cone spindle CPA-40Z.<sup>26</sup> The O<sub>2</sub>-Hb/PolyHb

equilibrium binding curves were measured by using a Hemox Analyzer (TCS Scientific Corp., New Hope, PA). The Hb/PolyHb kinetics of O<sub>2</sub> offloading ( $k_{off,O_2}$ ) and NO dioxygenation kinetics ( $k_{ox,NO}$ ) were measured with an Applied Photophysics SF-17 microvolume stopped-flow spectrophotometer (Applied Photophysics Ltd., Surrey, United Kingdom) using protocols previously described by Rameez and Palmer.<sup>27-29</sup> The MW distribution was estimated by using an Acclaim SEC-1000 column (Thermo Scientific, Waltham, MA) connected to a Thermo Scientific Dionex Ultimate UHPLC system using previously described methods.<sup>14,30</sup> All measurements were taken from the same sample used in the animal study.

### **ApoHb purification and biophysical properties**

The apoHb used in this study was produced by using acidified-ethanol coupled tangential flow filtration, as described previously.<sup>22</sup> The heme-binding site activity of the resulting apoHb was quantified with a dicyanohemin assay.<sup>21</sup> The total amount of protein in solution was estimated based on the molar extinction coefficient of apoHb.<sup>22</sup>

### **Hp purification and biophysical properties**

The Hp used for this study was purified from human Cohn fraction IV derived from pooled human plasma.<sup>31</sup> The resulting Hp contained both Hp2-1 and Hp2-2 phenotypes. The total amount of protein in solution was estimated by using a Bradford assay.<sup>32</sup> The Hb-binding capacity of Hp was assessed by monitoring Hb binding to Hp at 413 nm with size exclusion high-performance liquid chromatography (SEC-HPLC) and was used to quantify the concentration of Hp. The reaction of Hp with either unmodified human Hb or PolyHb synthesized in this study was monitored by using an SX-20 stopped-flow spectrophotometer using previously described methods (Applied Photophysics, Leatherhead, United Kingdom).<sup>12,14,33</sup> Excess Hp (2:1, Hp:PolyHb on a Hb tetramer binding basis) was allowed to react with PolyHb to form the resulting Hp-PolyHb complex. The resulting changes in size distribution after Hp binding was estimated with SEC-HPLC by using previously described methods.<sup>14,30</sup> All measurements were taken from the same sample used in the animal study.

### **Animal model**

Animal handling and care procedures were in accordance with the 2011 National Institutes of Health Guide for the Care and Use of Laboratory Animals. The University of California San Diego Institutional Animal Care and Use Committee approved the experimental protocol. In vivo evaluation of apoHb-Hp detoxification of PolyHb was performed on 55 to 65 g male Golden Syrian Hamsters (Charles River Laboratories, Boston, MA) fitted with a dorsal skinfold window chamber as previously described.<sup>34-36</sup> Animals were considered suitable for experiments if systemic parameters were as follows: heart rate (HR) >340 beats/min, MAP >80 mm Hg, systemic hematocrit >45%, and arterial O<sub>2</sub> partial pressure >50 mm Hg. In addition, animals with signs of low perfusion, inflammation, edema, or bleeding in their microvasculature were excluded from the study. Before treatment, baseline systemic parameters and microvascular hemodynamics were assessed. Animals were first treated with either: (1) 0.1 mL 0.9 wt% saline; (2) 0.1 mL apoHb (24.5 mg/L); or (3) 0.1 mL apoHb (24.5 mg/L) with 0.05 mL Hp (46.5 mg/mL). Twenty minutes after the initial treatment, systemic parameters and microvascular

hemodynamics were assessed. Afterward, the animals underwent a 20% isovolemic exchange transfusion with a 10 g/dL PolyHb solution. After another 20 minutes, systemic parameters and microvascular hemodynamics were measured. MAP and HR were monitored continuously (MP150; BIOPAC Systems, Inc., Santa Barbara, CA). The sample size of 5 animals per group was calculated based on an expected 10% difference in MAP between groups,  $\alpha = 0.05$ ,  $1 - \beta = 0.1$ , and equal enrollment for all groups. In addition, microhemodynamic measurements contain data from multiple vessels within the field (5-7 arterioles and venules selected at baseline based on visual clarity), improving the power of these measurements.

Each experiment is a repeated measures study, and thus all experimental time points are replicated between all animals and groups. Furthermore, each experimental group contains animals from multiple litters, improving the replication and randomization of these studies. Animals were randomly assigned to their respective group before baseline measurements were taken. Investigators were not blinded to group allocation during data collection or analysis. Blinding is not possible with these solutions as they have distinct colors. Blinding should have had little impact, however, because the measurements taken are highly quantitative.

### **Intravital microscopy**

The unanesthetized animal was placed in a restraining tube with a longitudinal slit from which the window chamber protruded, then fixed to the microscopic stage for transillumination with the intravital microscope (BX51WI; Olympus, New Hyde Park, NY). Animals were given 20 minutes to adjust to the tube environment, and images were obtained by using a CCD camera (4815; COHU, Inc., San Diego, CA). Measurements were performed by using a 40× (LUMPFLL-WIR; numerical aperture, 0.8; Olympus) water immersion objective.

### **Microvascular hemodynamics**

Arteriolar and venular blood flow velocities were measured by using the photodiode cross-correlation method (Photo Diode/Velocity; Vista Electronics, San Diego, CA).<sup>37</sup> The measured centerline velocity ( $V$ ) was corrected according to blood vessel size to obtain the mean RBC velocity.<sup>38</sup> A video image-shearing method was used to measure blood vessel diameter ( $D$ ).<sup>39</sup> Blood flow ( $Q$ ) was calculated from the measured values as

$$Q = \pi \times V \left( \frac{D}{2} \right)^2.$$

### **Functional capillary density**

Functional capillaries, defined as capillary segments that have RBC transit of at least one RBC in a 60-second period in 10 successive microscopic fields, were assessed in a region of 0.46 mm<sup>2</sup>. FCD (mm<sup>-1</sup>) was calculated as the total length of RBC-perfused capillaries divided by the area (0.46 mm<sup>2</sup>).

### **Ethics statement**

Golden Syrian hamsters were anesthetized with ketamine/xylazine (ketamine, 200 mg/kg; xylazine, 10 mg/kg) for surgical instrumentation. All animals were euthanized with sodium pentobarbital (300 mg/kg). All experimental protocols used to handle these animals were approved by the University of California San Diego

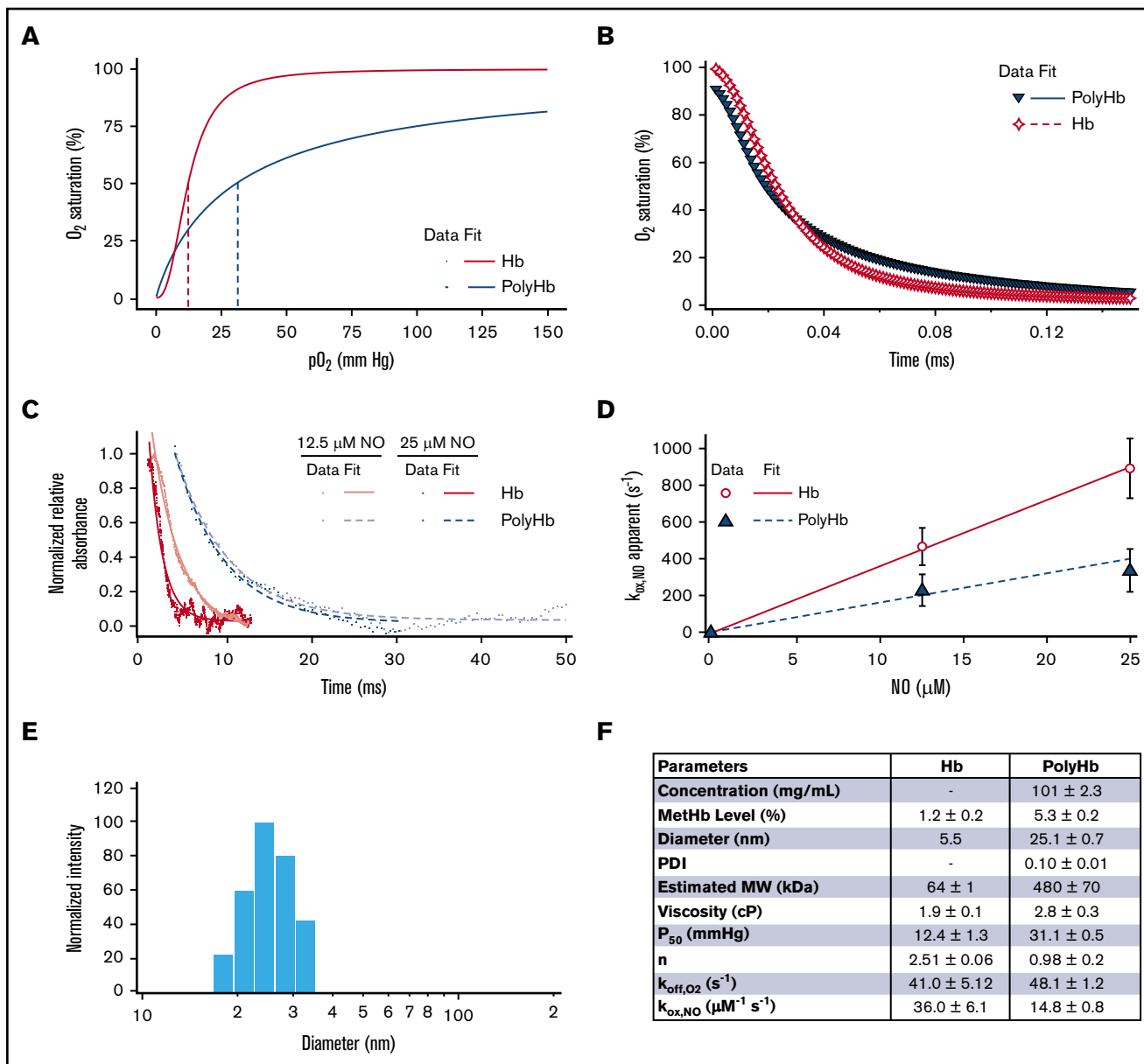


**Figure 2. Biophysical properties of the PolyHb used in this study.** (A) O<sub>2</sub> equilibrium curves for PolyHb and Hb with 3 runs per sample. (B) Comparison of the time course for deoxygenation in the presence of 1.5 mg/mL sodium dithionite for oxygenated Hb and PolyHb. For deoxygenation, the reactions were monitored at 437.5 nm and 20°C in 0.1 M pH 7.4 phosphate-buffered saline. (C) Time courses for the NO dioxygenation reaction with oxygenated Hb and PolyHb at NO 12.5 μM and 25 μM. Dots represent experimental data, and the corresponding solid lines of the same color represent curve fits to the data. NO dioxygenation reactions were monitored at 420.0 nm and 20°C in 0.1 M pH 7.4 phosphate-buffered saline. (D) Comparison of the NO dioxygenation rates for Hb and PolyHb. For kinetics, the data show an average of 10 kinetic traces for each sample. The error bars indicate the standard deviation from 10 replicates. (E) Representative intensity distributions of the hydrodynamic diameter of PolyHb. (F) Summary of the biophysical properties of unmodified Hb and PolyHb.

Institutional Animal Care and Use Committee. The Hb used to prepare these materials was purified from expired RBCs donated from The Ohio State University Wexner Medical Center (Columbus, OH). The Hp used in this study was purified from Cohn fraction IV paste purchased from Seraplex, Inc. (Pasadena, CA).

### Statistical analysis

Results are presented as mean ± standard deviation. One-way analysis of variance was used to analyze data within the same

group. All box plots are presented with the median on the centerline; the box limits are set to the upper (75%) and lower (25%) quartiles. All outliers are shown in each plot. Post hoc analysis was completed with the Dunn multiple comparison test. Data between groups were analyzed with a 2-way analysis of variance with Bonferroni tests. When possible, in vivo data were compared against baseline in the same animal or same vessel as a ratio relative to the baseline. All statistical calculations and data analyses were performed with R version 3.6.2 (R Foundation for

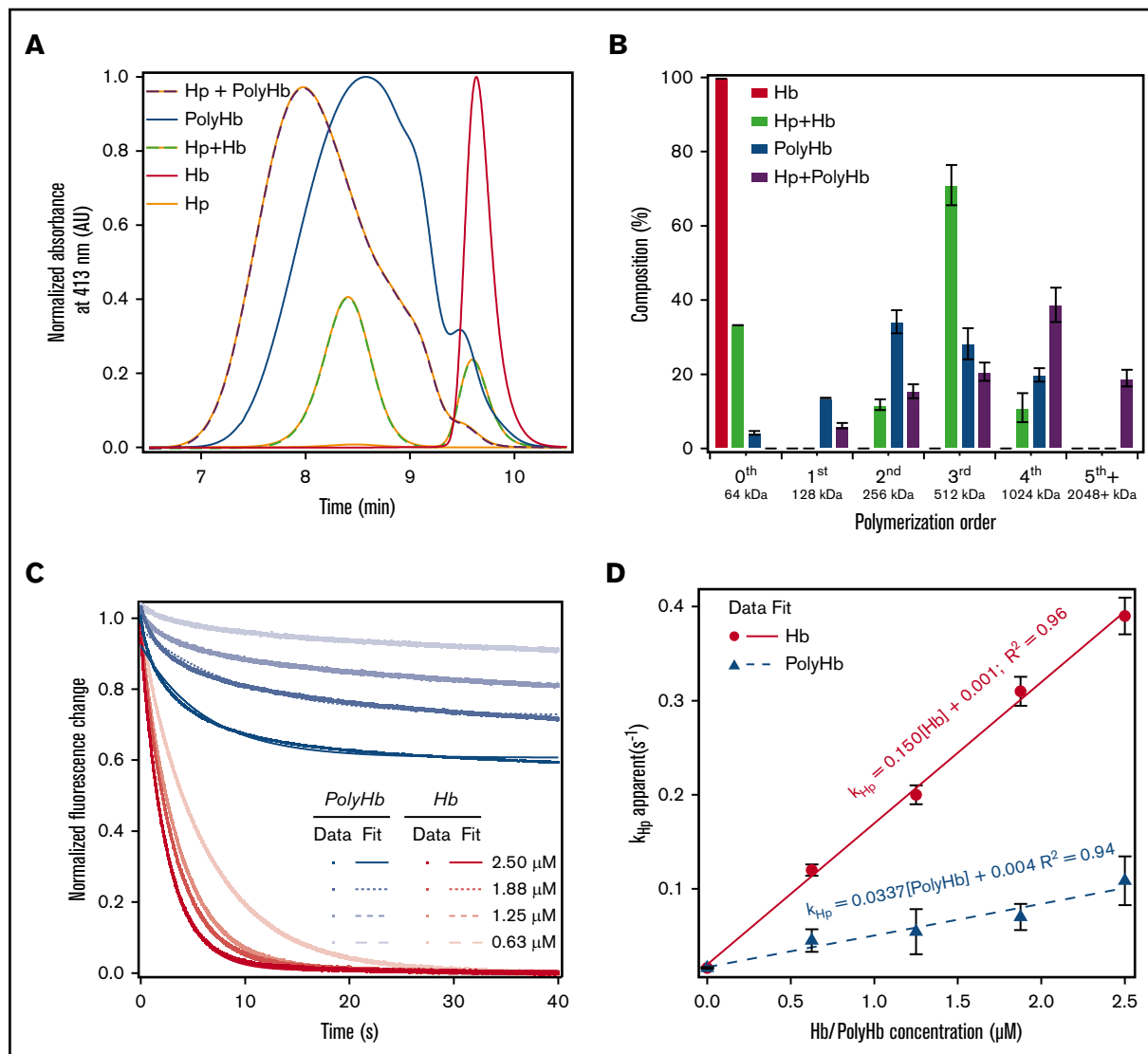


**Figure 3. SEC-HPLC and rapid kinetics of Hp binding to Hb and PolyHb.** (A) SEC-HPLC chromatograms of Hb and PolyHb with and without Hp. The absorbance was monitored at 413 nm to detect heme. The peak for unmodified Hb elutes at ~9.6 minutes. Each chromatogram was normalized to the peak area under the curve before the addition of Hp. The molar ratio of Hb to Hp was 1.5:1; the molar ratio of PolyHb to Hp was 1:2. (B) The percent composition based on the approximate size order was determined with a Gaussian deconvolution of the resulting chromatograms. (C) Time courses of Hp (0.25 μM, Hb tetramer binding basis) and Hb/PolyHb (on an Hb tetramer molar basis) were fit to monoexponential equations (dashed lines). Experimental data show an average of 10 kinetic traces. The reactions were monitored by the fluorescence emission using a 310 nm high-pass filter at 20°C. Phosphate-buffered saline (0.1 M, pH 7.4) was used as the reaction buffer. (D) Second-order rate constants of Hp binding to Hb/PolyHb derived as a function of Hb concentration on a Hb tetramer molar basis.

Statistical Computing). For all tests,  $P < .05$  was considered statistically significant.

## Results

### PolyHb characterization

A summary of the biophysical properties of the PolyHb used in this study is shown in Figure 2. Polymerization significantly increased the methHb level ( $5.3\% \pm 0.2\%$ ) compared with unmodified Hb ( $1.2\% \pm 0.2\%$ ). The PolyHb used in this study had significantly reduced  $O_2$  affinity ( $P_{50} = 31.1 \pm 0.5$  mm Hg) and reduced cooperativity ( $n = 0.98 \pm 0.21$ ) compared with the  $O_2$  affinity ( $P_{50} = 12.4 \pm 1.3$  mm Hg) and cooperativity ( $n = 2.51 \pm 0.06$ ) of unmodified Hb. After polymerization,

the hydrodynamic diameter of PolyHb increased to 25.1 nm. The resulting PolyHb solution had a single peak with a low polydispersity index ( $0.10 \pm 0.10$ ). PolyHb had an estimated average MW of 480 kDa. Polymerization significantly increased the viscosity ( $2.8 \pm 0.3$  cP) compared with unmodified Hb ( $1.2 \pm 0.2$  cP). Polymerization significantly increased the rate of  $O_2$  offloading ( $k_{off,O_2} = 48.1 \pm 1.2$ ) compared with unmodified Hb ( $k_{off,O_2} = 41.0 \pm 5.12$ ). In contrast, polymerization significantly decreased the rate of NO dioxygenation ( $k_{ox,NO} = 14.8 \pm 0.8$ ) compared with unmodified Hb ( $k_{ox,NO} = 36.0 \pm 6.1$ ).

### Characterization of Hp binding to PolyHb

The effect of Hp binding on the size distribution of PolyHb and Hb is shown in Figure 3A. To verify that Hp completely bound to

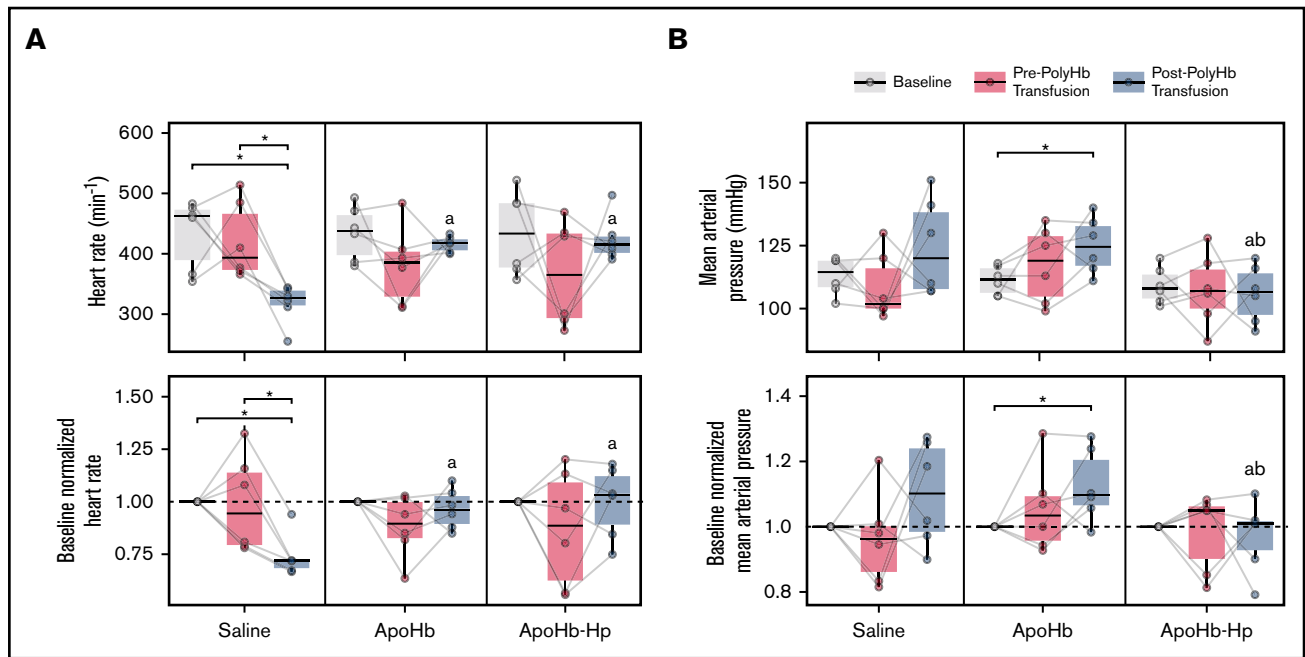


**Figure 4. Systemic hemodynamics measured throughout the study.** HR (A) and MAP (B) measured at baseline, after administration of saline, apoHb, or apoHb-Hp, and after 20% isovolemic exchange transfusion of PolyHb. Top panels show the measured values; bottom panels show values normalized to the baseline of the same animal. Gray lines connect measurements obtained in the same animal. \* $P < .05$  compared between groups. <sup>a</sup> $P < .05$  compared with the saline administration group at the same time point. <sup>b</sup> $P < .05$  compared with apoHb administration group at the same time point.  $n = 5$  animals per group.

unmodified Hb, excess Hb was mixed with Hp at a 3:2 molar ratio of Hb to Hp. The central peak for Hb was observed at an elution time of  $9.61 \pm 0.05$  minutes. Hp was slightly larger, with an average elution time of  $8.32 \pm 0.12$  minutes. Compared with Hp and Hb, PolyHb had a relatively broad size distribution. Due to this broad size distribution, a polymer size order decomposition was performed on the resulting peaks to estimate the composition of the Hp polymer species. The results of this analysis are shown in Figure 3B. After mixing the 3:2 molar ratio of Hb to Hp, 33% of unmodified Hb (size order 64 kDa) remains unbound. This finding indicates that all of the Hp in solution was able to bind Hb. The resulting Hp-Hb complex was  $\sim 512$  kDa in size, which indicates that a single bound Hp increases the size by at least 500 kDa. Analysis of LMW PolyHb fractions ( $< 512$  kDa) indicates that only 10% of PolyHb does not bind to Hp. However, the 64 kDa zero-order PolyHb species is completely eliminated by Hp binding. The large MW (1 and 2 MDa) polymer size orders increase by 30%. Representative time courses of the kinetics of Hp binding to Hb and PolyHb are shown in Figure 3C. The dependence of the pseudo first-order rates on Hb/PolyHb concentration is shown in Figure 3D. Overall, the kinetics of Hp binding to Hb was much faster ( $0.150 \pm 0.001 \mu\text{M}^{-1}\text{s}^{-1}$ ) compared with PolyHb ( $0.0337 \pm 0.001 \mu\text{M}^{-1}\text{s}^{-1}$ ).

### Systemic hemodynamics

MAP and HR measurements from throughout the experimental study are shown in Figure 4. There was no significant difference in baseline conditions for any of the animals. Before transfusion of PolyHb, administration of saline, apoHb, and apoHb-Hp had no significant effect on MAP or HR compared with each other and the baseline condition. After exchange transfusion of PolyHb in animals that underwent treatment with saline, there was a significant decrease

in HR compared with baseline and pretransfusion conditions. For animals that were administered apoHb, there was a significant increase in MAP. For animals that underwent treatment with apoHb-Hp, there was no significant change in MAP or HR compared with baseline and pretransfusion conditions. In animals administered the apoHb-Hp solution, the post-PolyHb transfusion HR was significantly higher compared with animals administered the saline solution. MAP in animals administered either saline or apoHb solutions after PolyHb transfusion was significantly higher compared with animals administered apoHb-Hp solutions.

### Microhemodynamics

Changes in arteriole and venule diameters as measured with intravital microscopy are shown in Figure 5. There was a significant decrease in the diameter of arterioles and venules compared with baseline after vehicle administration and PolyHb transfusion in the saline treatment group. For animals in the apoHb treatment group, there was a significant decrease in relative arteriole and venule diameters compared with baseline after transfusion of PolyHb. For animals in the apoHb-Hp treatment group, there were no significant changes observed in arteriole and venule diameters throughout treatment. The vessel diameters of venules and arterioles in the apoHb-Hp group were significantly larger compared with the saline treatment group.

Changes in the blood velocity and volumetric flow rate measured via intravital microscopy are shown in Figure 6. The relative arteriole and venule fluid velocity in the saline group significantly increased after PolyHb transfusion. In contrast, the relative venule fluid velocity significantly decreased after apoHb administration. The venule fluid velocities in the apoHb treatment group were significantly lower

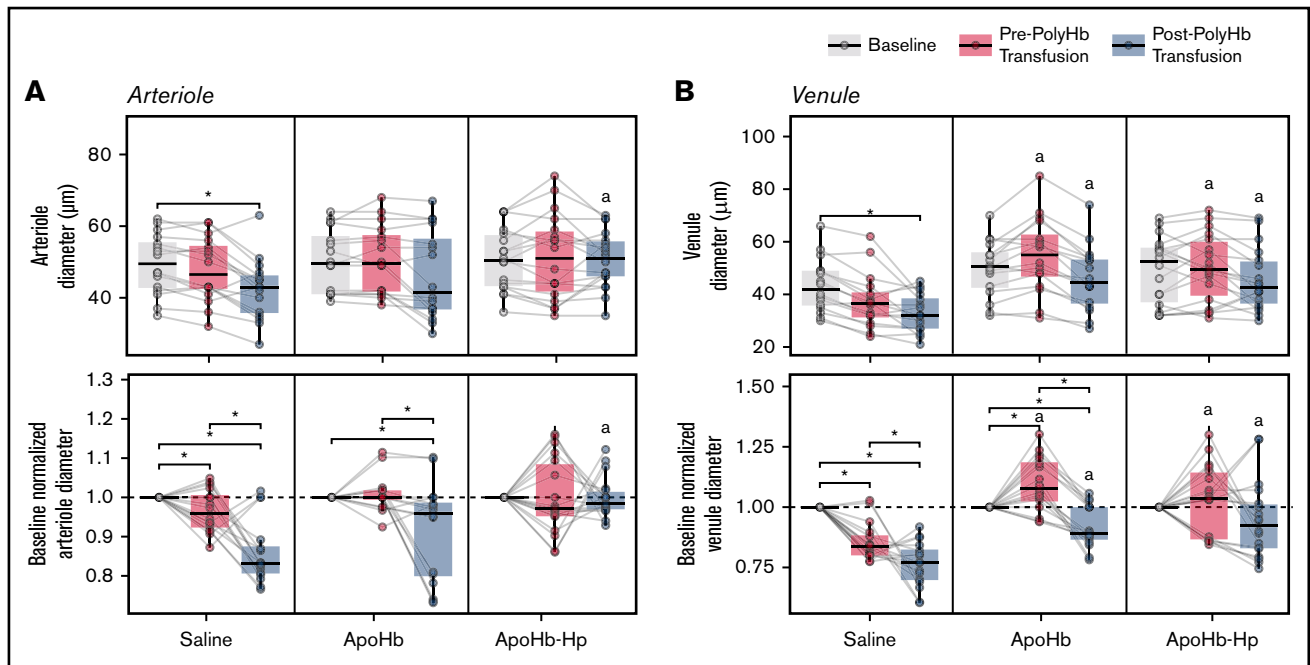


**Figure 5. Diameters of blood vessels measured with intravital microscopy.** Arteriole (A) and venule (B) diameters measured at baseline; after administration of saline, apoHb, or apoHb-Hp; and after 20% isovolemic exchange transfusion of PolyHb. Top panels show the measured values; bottom panels show values normalized to the baseline of the same vessel in the same animal. Gray lines connect measurements obtained in the same blood vessel. \* $P < .05$  compared between groups. <sup>a</sup> $P < .05$  compared with the saline administration group at the same time point.  $n = 5$  animals per group, 6 vessels per animal.

than the venule fluid velocities in the saline treatment group. After treatment with apoHb, we observed a significant decrease in the arteriole volumetric flow rate. In the saline and apoHb treatment groups, the volumetric flow rate in the arterioles and venules decreased after PolyHb transfusion.

In the apoHb-Hp treatment group, there were no significant changes in arteriole and venule fluid velocities and volumetric flow rates throughout the study. The venule fluid velocity in the apoHb-Hp treatment group was significantly lower than in the saline group and significantly higher than in the apoHb treatment group. The arteriole and venule volumetric flow rates after PolyHb administration in the apoHb-Hp group were significantly higher compared with the saline and apoHb treatment groups.

Changes in FCD throughout the intravital microscopy study are presented in Figure 7. After treatment with saline, the FCD significantly decreased relative to baseline. In contrast, treatment with apoHb resulted in a significant increase in FCD. After PolyHb transfusion, FCD significantly decreased in the saline and apoHb treatment groups. There were no significant changes in FCD in the apoHb-Hp treatment group compared with baseline. After PolyHb transfusion, the FCD in the apoHb-Hp treatment group was significantly higher than the FCD in the saline and apoHb treatment groups. There were no significant differences at baseline between treatment groups for any microhemodynamic parameters.

## Discussion

The principal finding of this study is that administration of an Hb and heme-scavenging material (apoHb-Hp) maintained hemodynamics after a 20% isovolemic exchange transfusion with LMW PolyHb. In animals administered apoHb-Hp, negligible changes in MAP, HR,

and microhemodynamics occurred compared with baseline conditions. Compared with the systemic and microcirculatory changes observed in the apoHb and saline groups, the relatively small changes in the apoHb-Hp group indicate that Hp-based species may serve as appropriate materials to counteract the vasoactive effects of LMW HBOCs that are capable of binding to Hp.

The biophysical properties of the Hp produced in this study were comparable to values reported in the literature. The rate constant for Hp binding to Hb was similar to values reported in the literature for Hb ( $0.129 \mu\text{M}^{-1}\text{s}^{-1}$ ).<sup>12,33</sup> The rate constant for Hp binding to PolyHb was much higher than the values reported in the literature for a PolyHb ( $0.003 \mu\text{M}^{-1}\text{s}^{-1}$ ) and Oxyglobin ( $0.011 \mu\text{M}^{-1}\text{s}^{-1}$ ; OPK Biotech, Cambridge, MA).<sup>12</sup> However, it was comparable to previously produced PolyHb.<sup>14</sup> Although the rate of Hp binding to PolyHb was significantly lower than the rate of Hp binding to Hb, systemic and microcirculatory hemodynamics were maintained throughout the studies. By observing the change in fluorescence intensity, we were able to calculate the percentage of PolyHb that is capable of binding to Hp. For Hb, we calculated complete Hp binding site saturation when excess Hb was in solution. In contrast, only a fraction of the Hp binding sites was saturated after excess PolyHb was added to the Hp solution. Despite only observing fractional Hp binding site saturation, we still observed dramatic increases in the MW and diameter of PolyHb after Hp was added. This finding indicates that Hp is likely capable of binding higher order (MW >64 kDa) PolyHb molecules. Thus, Hp likely has a role in compartmentalizing zero-, first, and second-order PolyHbs in the circulation.

The  $\text{O}_2$  affinity of the LMW PolyHb used in this study ( $31.1 \pm 0.5$  mm Hg) was similar to the  $\text{O}_2$  affinity of Hb in human RBCs



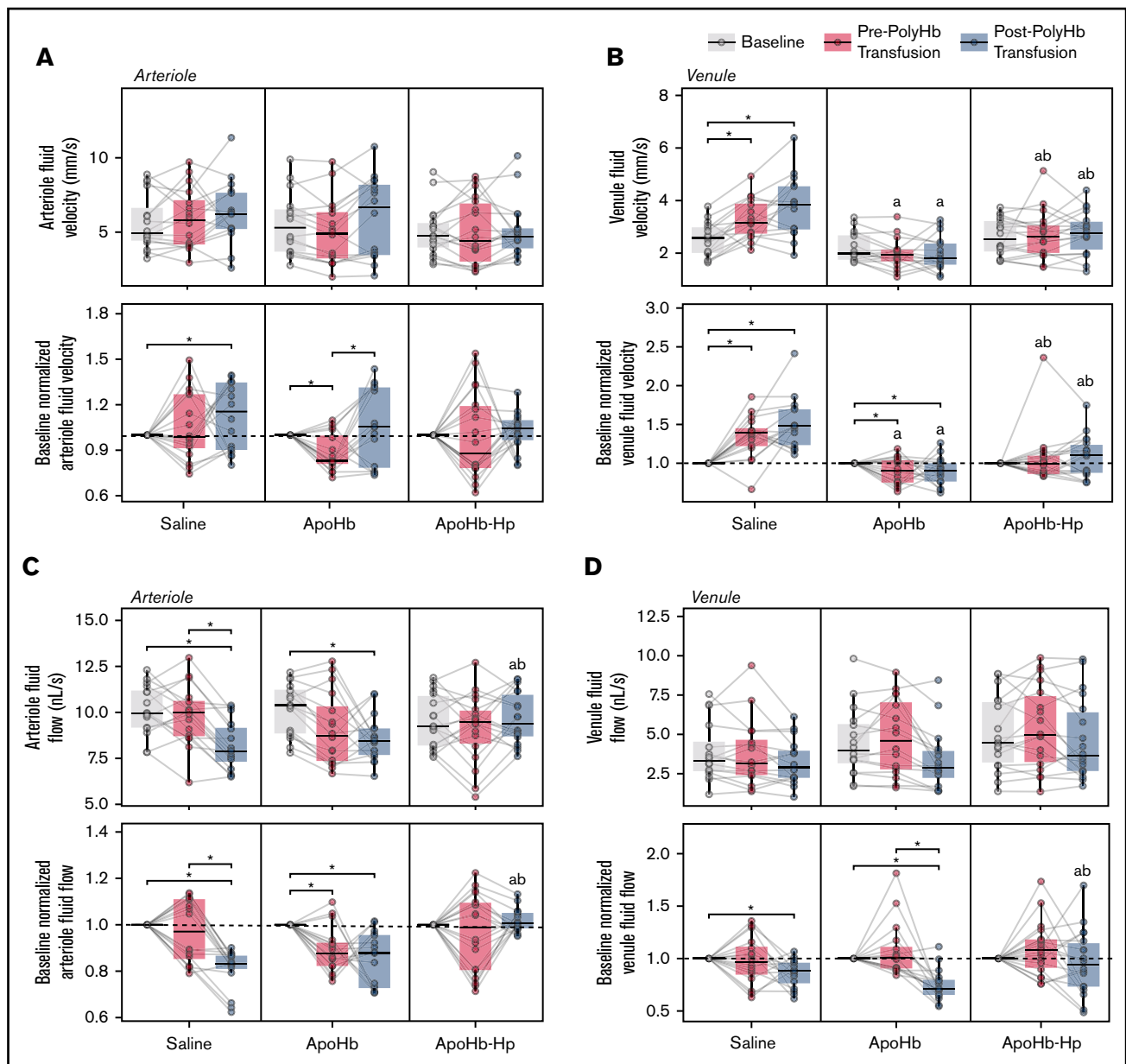


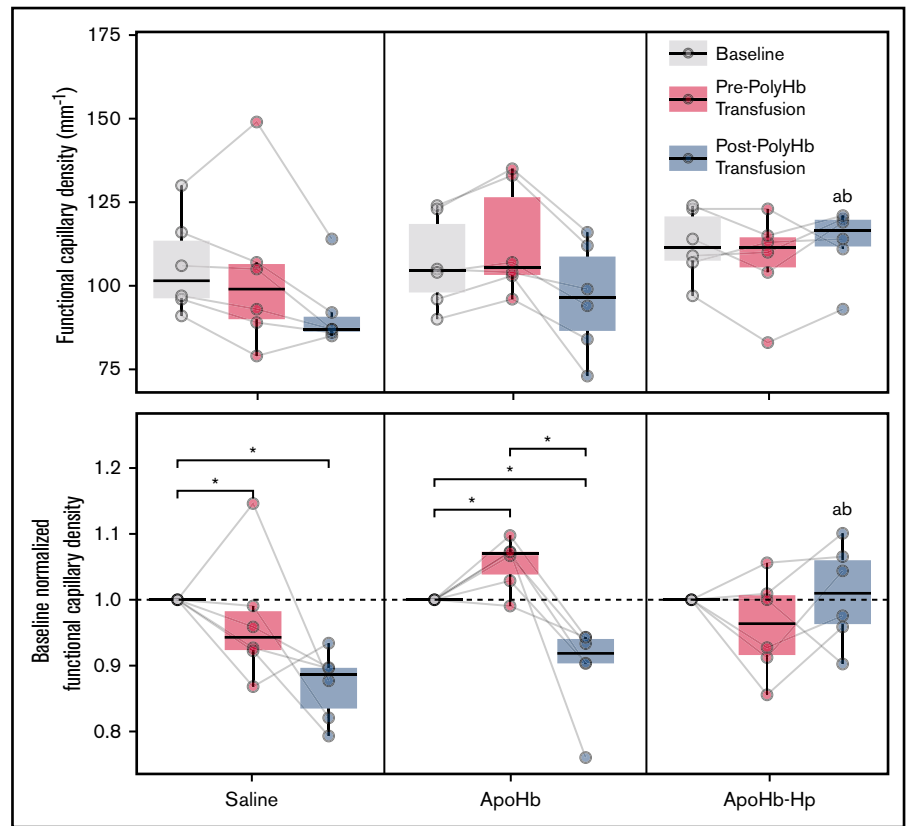
**Figure 6. Blood velocity and flow rates in blood vessels measured with intravital microscopy.** Arteriole (A) and venule (B) flow velocities measured at baseline; after administration of saline, apoHb, or apoHb-Hp; and after 20% isovolemic exchange transfusion of PolyHb. Arteriole (C) and venule (D) volumetric flow rates are also shown at the same conditions. Top panels show the measured values; bottom panels show values normalized to the baseline of the same vessel in the same animal. Gray lines connect measurements in the same blood vessel. \* $P < .05$  compared between groups. <sup>a</sup> $P < .05$  compared with the saline administration group at the same time point. <sup>b</sup> $P < .05$  compared with the apoHb administration group at the same time point.  $n = 5$  animals per group, 6 vessels per animal.

( $P_{50} = 29.3$ ).<sup>40</sup> Although the  $P_{50}$  was similar to Hb in RBCs, the lack of cooperativity ( $n = 0.98 \pm 0.2$ ) likely results in changes to  $O_2$  offloading in the arterioles. The  $O_2$  affinity was also comparable to previously produced PolyHbs ( $P_{50} = 30.7 \pm 1.2$  mm Hg)<sup>14,41</sup> and PolyHeme ( $P_{50} \sim 29$  mm Hg).<sup>42</sup> Despite the fact that the average MW and diameter of the PolyHb produced for this study (average MW, 480 kDa) are significantly greater than those of previously produced commercial products (PolyHeme, 64-400 kDa [average, 150 kDa]; HBOC-201, 69-500 kDa [average, 250 kDa]),<sup>6</sup> the PolyHbs produced in this study are composed of  $\sim 50\%$  LMW species (MW  $< 500$  kDa),

which are known to be more vasoactive than the higher MW species.<sup>43</sup>

The relative changes in MAP and vessel tone compared with baseline in the saline treatment group were, on average, comparable to the changes observed after a top-load dose of HBOC-201.<sup>44</sup> This outcome was expected, given that the LMW PolyHb molecules used in this study had similar size distributions and  $O_2$  affinity compared with HBOC-201. The relatively similar properties of the PolyHb produced for this study make it a promising surrogate for previous commercial products.

**Figure 7. FCD measured at baseline; after administration of saline, apoHb, or apoHb-Hp; and after 20% isovolemic exchange transfusion of PolyHb.** Top panels show the measured values; bottom panels show values normalized to the baseline FCD of the same animal. Gray lines connect measurements obtained in the same animal. \* $P < .05$  compared between groups. <sup>a</sup> $P < .05$  compared with the saline administration group at the same timepoint. <sup>b</sup> $P < .05$  compared with the apoHb administration group at the same time point.  $n = 5$  animals per group.



Administration of apoHb alone had relatively little effect on maintaining hemodynamics after transfusion of PolyHb. In many cases, apoHb administration resulted in similar changes relative to baseline compared with the saline treatment group. This finding was expected, given that the rate of heme release from PolyHbs is relatively low compared with stroma free Hb.<sup>12</sup> More importantly, because apoHb exists as an  $\alpha\beta$  dimer (32 kDa), we expect it to be rapidly cleared through the kidneys within 5 minutes to 1 hour after administration.<sup>45,46</sup> Moreover, heme binding to apoHb yields methHb, which can cause oxidative tissue injury. However, the circulatory half-life would be increased if the apoHb were to bind plasma Hp. In addition, heme binding to apoHb bound to Hp would neutralize the effects of free heme. Interestingly, the HR significantly decreased after PolyHb transfusion in the saline treatment group. This effect did not occur in the groups administered the apoHb or apoHb-Hp solutions.

In contrast to both apoHb and saline, the apoHb-Hp complex was successful at maintaining baseline hemodynamics after transfusion of PolyHb. This indicates that Hp likely can mitigate the pressor effect of PolyHb by compartmentalizing LMW PolyHb within the vascular lumen. This mechanism is likely similar to the previously reported mechanism of cell-free Hb localization that preserved NO signaling.<sup>19</sup> By increasing the MW of PolyHb via exchange of apoHb in the apoHb-Hp complexes with PolyHb, and thus eliminating the presence of small PolyHb species, translocation of PolyHb may be effectively stopped.

Previous studies have attempted to counteract the pressor effect of HBOCs via coadministration of adenosine or nitroglycerin.<sup>7</sup> However, these materials require careful control of the dose to

avoid hypotension. In contrast, independent administration of the apoHb-Hp solution did not significantly decrease MAP or alter HR compared with baseline conditions. Unlike methods that target NO or endothelin, apoHb-Hp scavenging directly targets LMW stroma free Hb species. The PolyHb used in this study was shown to be vasoactive in other species (guinea pigs), and reduction of the LMW PolyHb species via diafiltration reduced the vasoactivity.<sup>10</sup> By targeting the LMW Hb species directly with apoHb-Hp and Hp, there is no need to balance a pressor response.

There are several limitations to this study. We administered the apoHb-Hp solution before performing the exchange transfusion with PolyHb. Because of this protocol, we were able to evaluate the effect of apoHb and the apoHb-Hp complex on hemodynamics. However, in the clinic, the Hp solution would likely be administered after PolyHb transfusion if elevated MAP were observed by the physician. Additional studies should instead examine the effect of apoHb-Hp administration after hypertension is induced with an LMW PolyHb. Finally, this study only evaluated a PolyHb that was capable of binding to Hp. It did not take into account chemically modified Hbs that do not bind to Hp, such as  $\alpha$ -crosslinked Hb.<sup>12,33</sup> In addition, in a clinical setting, the transfusion volume can vary from 10% to 95% of the total blood volume.<sup>47</sup> This preliminary study only examined a single-dose volume of the PolyHb solution. Future studies should examine the relative effectiveness of the apoHb-Hp complex after transfusion of larger volumes of PolyHb and explore the long-term consequences of the apoHb-Hp complex in other manifestations of acellular Hb toxicity beyond vasoactivity. Unfortunately, the results of this study cannot be directly extrapolated to humans, and additional preclinical studies in other species with

different vasoactive mechanisms should be explored, including guinea pigs<sup>10</sup> and lambs,<sup>48</sup> to supplement the current investigation of the microcirculation in the window chamber model.

In conclusion, the results of this study indicate that the apoHb-Hp complex is a promising biomaterial that may make HBOCs safer for clinical application via mitigation of the pressor effect.

## Acknowledgments

The authors thank Cynthia Walser (University of California San Diego) for assistance with surgical preparation of the animals.

This work was supported by grants from the National Institutes of Health, National Heart, Lung, and Blood Institute (R56HL123015, T32-HL105373, R01HL126945, and R01HL138116) and National Institute of Biomedical Imaging and Bioengineering (R01EB021926), The Ohio State University Office of Undergraduate Research & Creative Inquiry Advanced Summer Research Fellowship, the Pelotonia Undergraduate Fellowship, and the Pelotonia Graduate Research Fellowship.

Any opinions, findings, and conclusions expressed in this material are those of the author(s) and do not necessarily reflect those of the Pelotonia Fellowship Program.

## Authorship

Contribution: D.A.B. wrote the main manuscript text and prepared the figures; D.A.B., C.M., I.S.P., and A.T.W. performed the experiments and analyzed the data; C.M., I.S.P., A.T.W., P.C., and A.F.P. reviewed and revised the manuscript; and all authors contributed to the design and implementation of the experiment.

Conflict-of-interest disclosure: I.S.P., A.F.P., and D.A.B. are inventors on a pending patent application outlining methods related to the production of proteins such as apoHb and Hp (PCT/US2020/016267). The remaining authors declare no competing financial interests.

ORCID profiles: D.A.B., 0000-0002-7633-6219; C.M., 0000-0003-4832-3661; I.S.P., 0000-0002-4035-0027; A.T.W., 0000-0003-2150-9263; P.C., 0000-0002-8794-2839.

Correspondence: Pedro Cabrales, Department of Bioengineering, University of California San Diego, 9500 Gilman Dr, La Jolla, CA 92093; e-mail: pcabrales@ucsd.edu; or Andre F. Palmer, William G. Lowrie Department of Chemical and Biomolecular Engineering, The Ohio State University, 452 CBEC, 151 W Woodruff Ave, Columbus OH 43210; e-mail: palmer.351@osu.edu.

## References

1. Baron DM, Franchini M, Goobie SM, et al. Patient blood management during the COVID-19 pandemic: a narrative review [published online ahead of print 27 April 2020]. *Anaesthesia*. doi:10.1111/anae.15095.
2. Gehrie EA, Frank SM, Goobie SM. Balancing supply and demand for blood during the COVID-19 pandemic [published online ahead of print 13 April 2020]. *Anesthesiology*. doi:10.1097/aln.0000000000003341.
3. Pagano MB, Hess JR, Tsang HC, et al. Prepare to adapt: blood supply and transfusion support during the first 2 weeks of the 2019 novel coronavirus (COVID-19) pandemic affecting Washington State. *Transfusion*. 2020;60(5):908-911.
4. Simonetti A, Ezzeldin H, Walderhaug M, Anderson SA, Forshee RA. An inter-regional US blood supply simulation model to evaluate blood availability to support planning for emergency preparedness and medical countermeasures. *Disaster Med Public Health Prep*. 2018;12(2):201-210.
5. Palmer AF, Intaglietta M. Blood substitutes. *Annu Rev Biomed Eng*. 2014;16(1):77-101.
6. Day TK. Current development and use of hemoglobin-based oxygen-carrying (HBOC) solutions. *J Vet Emerg Crit Care (San Antonio)*. 2003;13(2):77-93.
7. Taverne YJ, de Wijs-Meijler D, Te Lintel Hekkert M, et al. Normalization of hemoglobin-based oxygen carrier-201 induced vasoconstriction: targeting nitric oxide and endothelin. *J Appl Physiol (1985)*. 2017;122(5):1227-1237.
8. Freilich D, Pearce LB, Pitman A, et al. HBOC-201 vasoactivity in a phase III clinical trial in orthopedic surgery subjects—extrapolation of potential risk for acute trauma trials. *J Trauma*. 2009;66(2):365-376.
9. Sakai H, Hara H, Yuasa M, et al. Molecular dimensions of Hb-based O(2) carriers determine constriction of resistance arteries and hypertension. *Am J Physiol Heart Circ Physiol*. 2000;279(3):H908-H915.
10. Williams AT, Muller CR, Eaker AM, et al. Polymerized hemoglobin with increased molecular size reduces toxicity in healthy guinea pigs. *ACS Appl Bio Mater*. 2020;3(5):2976-2985.
11. Alayash AI. Mechanisms of toxicity and modulation of hemoglobin-based oxygen carriers. *Shock*. 2019;52(suppl 1):41-49.
12. Meng F, Kassa T, Jana S, et al. Comprehensive biochemical and biophysical characterization of hemoglobin-based oxygen carrier therapeutics: all HBOCs are not created equally. *Bioconjug Chem*. 2018;29(5):1560-1575.
13. Baek JH, Zhou Y, Harris DR, Schaer DJ, Palmer AF, Buehler PW. Down selection of polymerized bovine hemoglobins for use as oxygen releasing therapeutics in a guinea pig model. *Toxicol Sci*. 2012;127(2):567-581.
14. Belcher DA, Cuddington CT, Martindale EL, Pires IS, Palmer AF. Controlled polymerization and ultrafiltration increase the consistency of polymerized hemoglobin for use as an oxygen carrier. *Bioconjug Chem*. 2020;31(3):605-621.
15. Fastenberg JH, Garzon-Muvdi T, Hsue V, et al. Adenosine-induced transient hypotension for carotid artery injury during endoscopic skull-base surgery: case report and review of the literature. *Int Forum Allergy Rhinol*. 2019;9(9):1023-1029.
16. Fahmy NR. Nitroglycerin as a hypotensive drug during general anesthesia. *Anesthesiology*. 1978;49(1):17-20.

17. Schaer DJ, Vinchi F, Ingoglia G, Tolosano E, Buehler PW. Haptoglobin, hemopexin, and related defense pathways-basic science, clinical perspectives, and drug development. *Front Physiol.* 2014;5:415.
18. Munoz CJ, Pires IS, Baek JH, Buehler PW, Palmer AF, Cabrales P. Apohemoglobin-haptoglobin complex attenuates the pathobiology of circulating acellular hemoglobin and heme. *Am J Physiol Heart Circ Physiol.* 2020;318(5):H1296-H1307.
19. Schaer CA, Deuel JW, Schildknecht D, et al. Haptoglobin preserves vascular nitric oxide signaling during hemolysis. *Am J Respir Crit Care Med.* 2016;193(10):1111-1122.
20. Schaer DJ, Buehler PW, Alayash AI, Belcher JD, Vercellotti GM. Hemolysis and free hemoglobin revisited: exploring hemoglobin and hemin scavengers as a novel class of therapeutic proteins. *Blood.* 2013;121(8):1276-1284.
21. Pires IS, Belcher DA, Palmer AF. Quantification of active apohemoglobin heme-binding sites via dicyanohemin incorporation. *Biochemistry.* 2017;56(40):5245-5259.
22. Pires IS, Belcher DA, Hickey R, et al. Novel manufacturing method for producing apohemoglobin and its biophysical properties. *Biotechnol Bioeng.* 2020;117(1):125-145.
23. Palmer AF, Sun G, Harris DR. Tangential flow filtration of hemoglobin. *Biotechnol Prog.* 2009;25(1):189-199.
24. Arifin DR, Palmer AF. Determination of size distribution and encapsulation efficiency of liposome-encapsulated hemoglobin blood substitutes using asymmetric flow field-flow fractionation coupled with multi-angle static light scattering. *Biotechnol Prog.* 2003;19(6):1798-1811.
25. Hawk PB. Blood analysis. In: Oser BL, ed. *Hawk's Physiological Chemistry*. 14th ed. New York, NY: McGraw-Hill Book Company; 1965:1090-1099.
26. Belcher DA, Ju JA, Baek JH, et al. The quaternary state of polymerized human hemoglobin regulates oxygenation of breast cancer solid tumors: a theoretical and experimental study. *PLoS One.* 2018;13(2):e0191275.
27. Rameez S, Palmer AF. Simple method for preparing poly(ethylene glycol)-surface-conjugated liposome-encapsulated hemoglobins: physicochemical properties, long-term storage stability, and their reactions with O<sub>2</sub>, CO, and NO. *Langmuir.* 2011;27(14):8829-8840.
28. Rameez S, Banerjee U, Fontes J, Roth A, Palmer AF. The reactivity of polymersome encapsulated hemoglobin with physiologically important gaseous ligands: oxygen, carbon monoxide and nitric oxide. *Macromolecules.* 2012;45(5):2385-2389.
29. Rameez S, Guzman N, Banerjee U, et al. Encapsulation of hemoglobin inside liposomes surface conjugated with poly(ethylene glycol) attenuates their reactions with gaseous ligands and regulates nitric oxide dependent vasodilation. *Biotechnol Prog.* 2012;28(3):636-645.
30. Cuddington C, Moses S, Belcher D, Ramesh N, Palmer A. Next-generation polymerized human hemoglobins in hepatic bioreactor simulations [published online ahead of print 10 January 2020]. *Biotechnol Prog.* doi: 10.1002/btpr.2958
31. Pires IS, Palmer AF. Tangential flow filtration of haptoglobin [published online ahead of print 29 April 2020]. *Biotechnol Prog.* doi: 10.1002/btpr.3010
32. Bradford MM. A rapid and sensitive method for the quantitation of microgram quantities of protein utilizing the principle of protein-dye binding. *Anal Biochem.* 1976;72(1-2):248-254.
33. Jia Y, Wood F, Buehler PW, Alayash AI. Haptoglobin preferentially binds  $\beta$  but not  $\alpha$  subunits cross-linked hemoglobin tetramers with minimal effects on ligand and redox reactions. *PLoS One.* 2013;8(3):e59841.
34. Cabrales P, Tsai AG, Frangos JA, Intaglietta M. Role of endothelial nitric oxide in microvascular oxygen delivery and consumption. *Free Radic Biol Med.* 2005;39(9):1229-1237.
35. Dufu K, Yalcin O, Ao-leong ESY, et al. GBT1118, a potent allosteric modifier of hemoglobin O<sub>2</sub> affinity, increases tolerance to severe hypoxia in mice. *Am J Physiol Heart Circ Physiol.* 2017;313(2):H381-H391.
36. Ortiz D, Barros M, Yan S, Cabrales P. Resuscitation from hemorrhagic shock using polymerized hemoglobin compared to blood. *Am J Emerg Med.* 2014;32(3):248-255.
37. Intaglietta M, Silverman NR, Tompkins WR. Capillary flow velocity measurements in vivo and in situ by television methods. *Microvasc Res.* 1975;10(2):165-179.
38. Lipowsky HH, Zweifach BW. Application of the "two-slit" photometric technique to the measurement of microvascular volumetric flow rates. *Microvasc Res.* 1978;15(1):93-101.
39. Intaglietta M, Tompkins WR. Microvascular measurements by video image shearing and splitting. *Microvasc Res.* 1973;5(3):309-312.
40. Patton JN, Palmer AF. Numerical simulation of oxygen delivery to muscle tissue in the presence of hemoglobin-based oxygen carriers. *Biotechnol Prog.* 2006;22(4):1025-1049.
41. Belcher DA, Banerjee U, Baehr CM, et al. Mixtures of tense and relaxed state polymerized human hemoglobin regulate oxygen affinity and tissue construct oxygenation. *PLoS One.* 2017;12(10):e0185988.
42. Napolitano LM. Hemoglobin-based oxygen carriers: first, second or third generation? Human or bovine? Where are we now? *Crit Care Clin.* 2009;25(2):279-301.
43. Cabrales P, Sun G, Zhou Y, et al. Effects of the molecular mass of tense-state polymerized bovine hemoglobin on blood pressure and vasoconstriction. *J Appl Physiol (1985).* 2009;107(5):1548-1558.
44. Song BK, Nugent WH, Moon-Massat PF, Pittman RN. Effects of a hemoglobin-based oxygen carrier (HBOC-201) and derivatives with altered oxygen affinity and viscosity on systemic and microcirculatory variables in a top-load rat model. *Microvasc Res.* 2014;95(1):124-130.
45. Matheson B, Razynska A, Kwansa H, Bucci E. Appearance of dissociable and cross-linked hemoglobins in the renal hilar lymph. *J Lab Clin Med.* 2000;135(6):459-464.

46. Kuna M, Mahdi F, Chade AR, Bidwell GL III. Molecular size modulates pharmacokinetics, biodistribution, and renal deposition of the drug delivery biopolymer elastin-like polypeptide. *Sci Rep.* 2018;8(1):7923.
47. Gould SA, Moore EE, Hoyt DB, et al. The life-sustaining capacity of human polymerized hemoglobin when red cells might be unavailable. *J Am Coll Surg.* 2002;195(4):445-452, NaN-455.
48. Yu B, Volpato GP, Chang K, Bloch KD, Zapol WM. Prevention of the pulmonary vasoconstrictor effects of HBOC-201 in awake lambs by continuously breathing nitric oxide. *Anesthesiology.* 2009;110(1):113-122.